# Effect of friction stir weld defects on fatigue lifetime of an Al-Cu-Li alloy

Thomas Le Jolu, Thilo F. Morgeneyer, Anne-Françoise Gourgues-Lorenzon

# Effect of friction stir weld defects on fatigue lifetime of an Al-Cu-Li alloy (AA-2198)

T. Le Jolu, T.F. Morgeneyer, A.F. Gourgues-Lorenzon
MINES ParisTech, Centre des Matériaux, CNRS UMR 7633, BP 87, 91003 Evry cedex, France

## ABSTRACT

The effect of Joint Line Remnant (JLR) on the fatigue lifetime of friction stir welds of a 2198 Al-alloy in T851 condition has been assessed experimentally by investigating "JLR-free" welds (welded in one sheet) and "JLR-bearing" welds (produced by welding 2 sheets with a natural oxide layer). A strong decrease in microhardness is found for the weakest weld zone together with a reduction in tensile properties compared to the base material, namely, 45% in yield strength and 22% in ultimate tensile strength. The fatigue strength of JLR-free and JLR-bearing welds at $10^5$ cycles (R=0.1) is reduced by 10% and 15% respectively compared to the base material. No obvious effect of JLR was evidenced concerning crack initiation mechanisms.

## KEYWORDS

Friction Stir Welding, Joint Line Remnant, Al-Cu-Li, S-N curves

## INTRODUCTION

The latest generation of Al-Cu-Li alloys is considered as candidate alloys for future aerospace applications thanks to their high density-to-strength ratio, good mechanical properties and corrosion resistance compared to other damage tolerant alloys [1-3]. Additionally, the requirement of weight and cost savings in the aircraft industry leads to increasing interest in joining processes to avoid riveting. Among them, Friction Stir Welding (FSW) is now emerging as a viable solid state process for joining aluminium alloys used in aerospace industry. The advantages of using this process are mainly the possibility to weld alloys traditionally considered as unweldable, the absence of defects such as porosity or cracks and the low distortion and residual stresses that may result from joining processes involving melting and solidification [4-6].

In recent studies, particular attention has been paid to a FSW defect in Al-alloys, which results from the natural oxide layer on butt surfaces, which is mixed during the welding process. It consists in a discontinuous line of oxide particles which crosses the weld thickness. It is commonly referred to in literature as `joint line remnant' (JLR), `lazy S', `zigzag curve' or 'zigzag line' [7-10]. When the defect is linked to the weld root it is also referred to as 'root flaw', 'kissing bond' or 'weak bond' [7, 11, 12]. It seems difficult to avoid JLR even using stable and optimized welding conditions [7, 11]. The bonding between the welded parts is often assessed via bending tests revealing that the kissing bond is the most detrimental defect and may lead to bending fracture initiation [7, 12, 13].

The influence of the JLR or kissing bond defect on the fatigue properties has been studied for various Al-alloys [7, 12-15]. Fatigue crack initiation may occur (although not systematically) at a JLR [15] or at a kissing bond-like defect [7, 12-14], but for others [10] no effect of the JLR is found. In all studies a reduction in fatigue lifetime of the FSW assembly with respect to the base material is found. In several studies a comparison with literature

results on supposedly defect-free welds is made, highlighting a strong reduction in fatigue strength (up to 50% [14]).

In the present study, the effect of JLR on the fatigue behaviour of 2198-T8 friction stir welds is assessed via testing sound welds (welded in one sheet) and welds with a JLR (obtained by joining two sheets with their natural oxide layer) while keeping reproducible welding and testing conditions.


## EXPERIMENTAL PROCEDURE

This study focuses on a 2198-T851 Al-Cu-Li alloy sheet of 3.1 mm in thickness. Its chemical composition is given in Table 1. In this paper the rolling direction will be referred to as L, the long transverse direction as T and the short transverse direction as S. Blanks cut from the sheet were joined by FSW by ONERA along the L direction using the welding parameters and tool geometry reported in Table 2. Two types of welds were produced: welds without JLR (referred to as "JLR-free" welds here) and welds containing a JLR defect. The JLR-free welds were produced via welding in one sheet. To make the JLR-bearing welds two sheets that were naturally oxidized before welding were joined. All welds were tested in the as-welded condition.

| | Al | Cu | Li | Ag | Mg | Zr | Fe | Si |
|---|---|---|---|---|---|---|---|---|
| Weight % | Bal. | 3.20 | 0.98 | 0.31 | 0.31 | 0.11 | 0.04 | 0.03 |

Table 1: Chemical composition of the 2198 alloy under study

| Travelling speed | Rotational speed | Pin diameter | Shoulder diameter |
|---|---|---|---|
| 480 mm/s | 1200 rpm | 4.2 mm | 13 mm |

Table 2:  Friction stir welding parameters and tool geometry

The grain structure of the base material and of the welds, and in particular the JLR defects were observed using polarized light optical microscopy after etching with a 3% HBF4 aqueous solution. The local mechanical properties of welds were assessed by $HV_{0.1}$ Vickers microhardness measurements on cross-weld polished sections, along lines parallel to the T direction, at various locations in the sheet thickness (0.5, 1.5 and 2.5 mm from the surface).

Tensile tests were carried out at room temperature using a 250 kN servo-hydraulic testing machine under displacement control with an initial strain rate of $2.10^{-4}$ $s^{-1}$. Tests were performed along L and T directions for the base material and along the T (cross-weld) direction for the welded joints. The geometry of tensile specimens is shown in Fig. 1. The weld line is located at the centre of the specimen and the initial gauge length of the longitudinal extensometer was 25 mm, i.e. about 2 times larger than the weld width.

Fatigue specimens were tested at room temperature along both L and T directions for the base material and along the cross-weld direction for the welded material. The fatigue tests were carried out using a servo-hydraulic testing machine with a load capacity of 250 kN. A sinusoidal load-time function was used, applying a stress ratio R of 0.1 and using a frequency of 20 Hz. The geometry of fatigue specimens for the base material and for the welded material is shown in Fig. 2 according to ASTM E-466-07 testing standard [16]. Before testing, specimens were ground at the corners to limit the stress concentrations and on the surfaces with 600 and 1200 SiC paper parallel to the loading direction. After the tests, fracture surfaces were examined using a LEO 1450 VP scanning electron microscope (SEM).
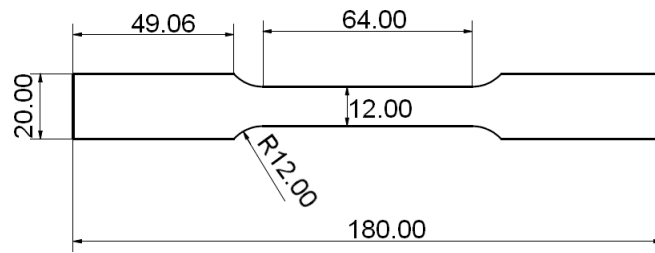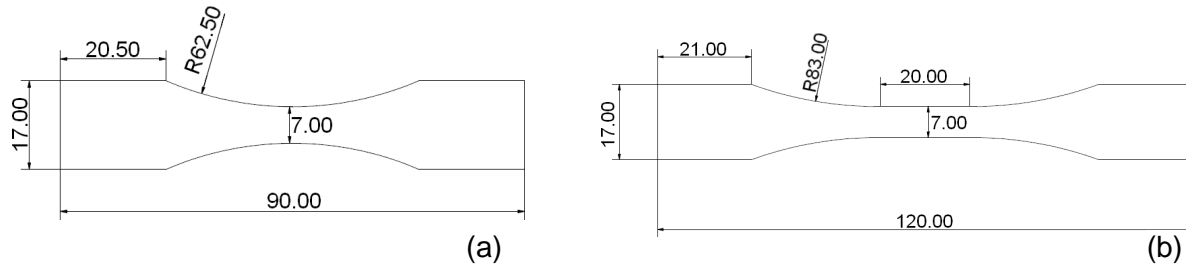
Fig. 1: Specimen geometry for tensile testing



(a)                                                                          (b)

Fig. 2: (a) Base material and (b) cross-weld specimen geometry for fatigue testing

## RESULTS

### Microstructure

The base material showed pancake shaped grains lying in the L-T plane (Fig. 3). Thicker recristallised grains were observed close to the sheet surfaces. Three zones were identified in the weld from optical microscopy observations (Fig. 4): the Weld Nugget (NG) is composed of fine equiaxed grains of typical size between 5 and 10 µm; the Thermo-Mechanically Affected Zone (TMAZ) is composed of highly deformed grains; the Heat Affected Zone (HAZ) has the same grain structure as the base material.
In the JLR-free weld (Fig. 4), no defect, such as JLR, porosity or cracks was observed at any weld location. In the material welded after natural oxidation, a JLR can be seen (Fig. 5) as a discontinuous zigzag curve of oxide particles through the sheet thickness.
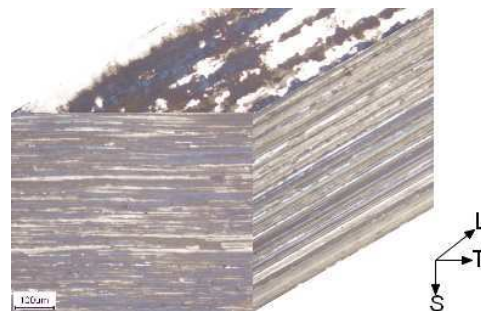


Fig. 3: Grain structure of the base material (montage of light optical micrographs)



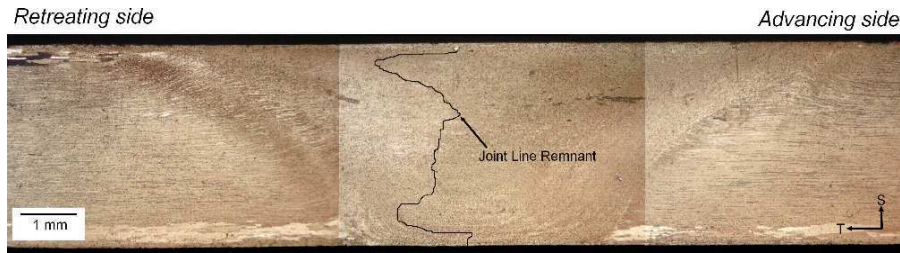Fig. 4: Light optical micrograph of a JLR-free weld

Fig. 5: Light optical micrograph of a JLR-bearing weld (JLR line redrawn artificially to highlight its morphology)

**Hardness and tensile properties**

The weld zone is softer than the base material (Fig. 6). At 10 mm from the centreline, hardness decreases down to a minimum in the weld nugget and the TMAZ (120 $HV_{0.1}$). The weld zone is softer by about 50 $HV_{0.1}$ than the base material. This difference is consistent with measurements made on welded T851 Al-Cu-Li alloys [17, 18]. A minimum in hardness is observed in the TMAZ on the retreating side at mid-thickness

Fig. 7a shows a slight anisotropy in tensile properties for the base material, namely, a 0.2% proof stress of 490 (resp. 470) MPa and a tensile strength of 530 (resp. 515) MPa for L and T directions, respectively, similarly to [3] but slighter than in [19]. Fig. 7b shows a tensile curve for the JLR-free weld. Note that elongation measurements only provide an averaged value over the entire weld. The amount of strain in the softer zones may be substantially higher. Yield stress and tensile strength of welded specimens are 255 MPa and 403MPa respectively, which means that the yield strength is almost half that of the base material. The work hardening capacity of the welded material is substantially higher than that of the base material. The joint efficiency, which is the ratio between the ultimate strength of the welded joint and that of the base material (along the T direction), is 78%, in agreement with [17]. However, as fracture could have occurred by strain localization, tensile strength and joint efficiency might also depend on specimen geometry. In the present study, fracture occurred in the weld nugget.
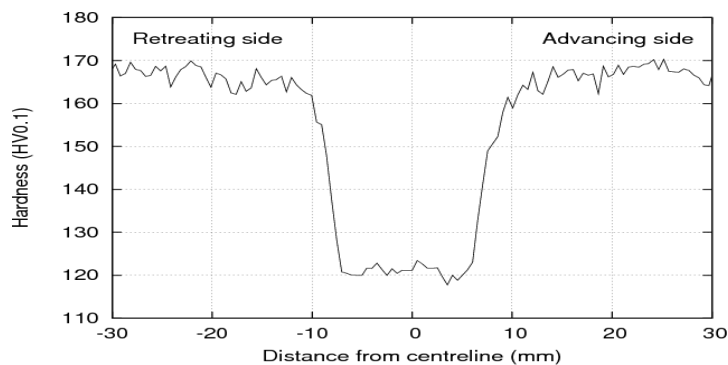


Fig. 6: Microhardness profiles across the weld for the JLR-bearing weld

**Fatigue properties**

Results of fatigue tests are reported in Fig. 8. The stress range corresponding to a fatigue lifetime of $10^5$ cycles will be considered here, i.e., the targeted lifetime for the aimed aircraft application. Its value is about 315 MPa for the base metal whatever the testing direction. This result differs from that of Cavaliere et al. [19], which found a difference in fatigue strength at $10^5$ cycles between the L and T directions of about 10%. However, the tensile anisotropy of their base material was also more pronounced than in the present study.
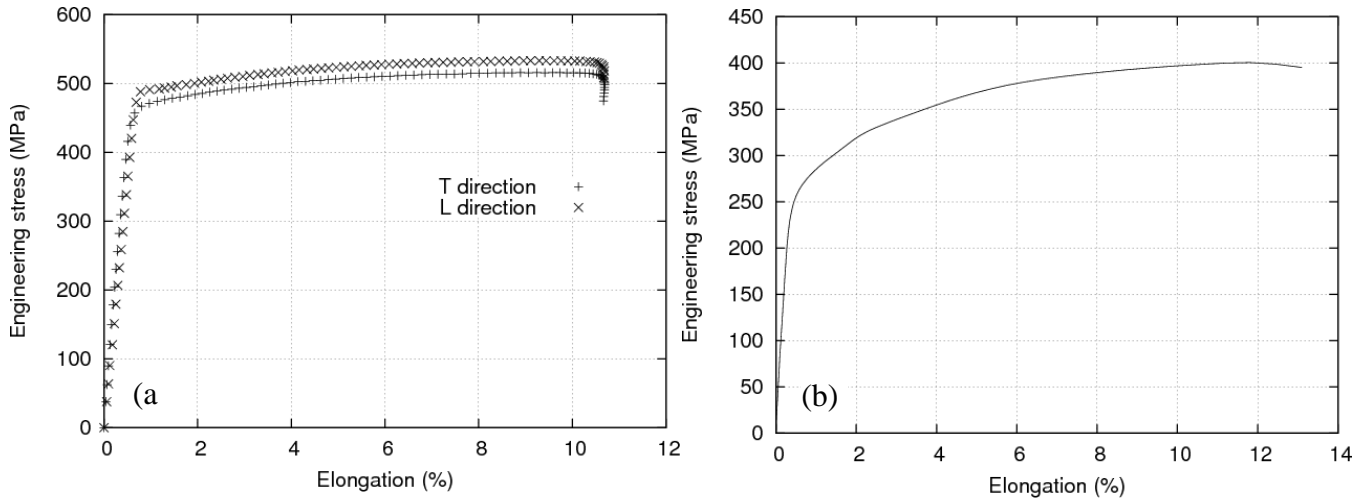
4

Fig. 7: Engineering tensile curves for (a) the base material and (b) a JLR-free cross-weld specimen

For JLR-free welds, the fatigue strength is about 290 MPa (i.e. a reduction by about 10% compared to the base material), whereas for JLR-bearing welds, the fatigue strength is about 270 MPa i.e. about 15% lower than for the base material. Thus, the reduction of fatigue lifetime due to the JLR defect is very limited in the current testing conditions. The same reduction (about 10%) was measured by Cavaliere et al. [19] at $3.10^5$ cycles for 2198-T8 base material tested along the T direction and 2198 FSW assemblies (R=0.33).

In order to identify the fatigue crack initiation area with respect to the JLR, the specimen shown in Fig. 9 was cut through the fatigue fracture zone (see dotted line), polished and etched (Fig. 10a), showing that the fatigue crack initiated within the WN. In other specimens, the fatigue crack initiated in the TMAZ/HAZ (Fig. 10b) or in the WN close to the JLR (Fig. 10c). In JLR-free welds, fatigue crack initiation took place in the TMAZ/HAZ for 4 specimens and in the WN for 3 specimens. 4 specimens of the JLR-bearing weld failed in the TMAZ/HAZ and 6 failed in the WN. Only for 3 specimens failed in the WN, the crack initiation region was close to the JLR, yet with no reduction in fatigue life (Fig. 8b). Note that half of the fatigue cracks initiated from a specimen corner (despite the grinding) without any difference between base material and welds.
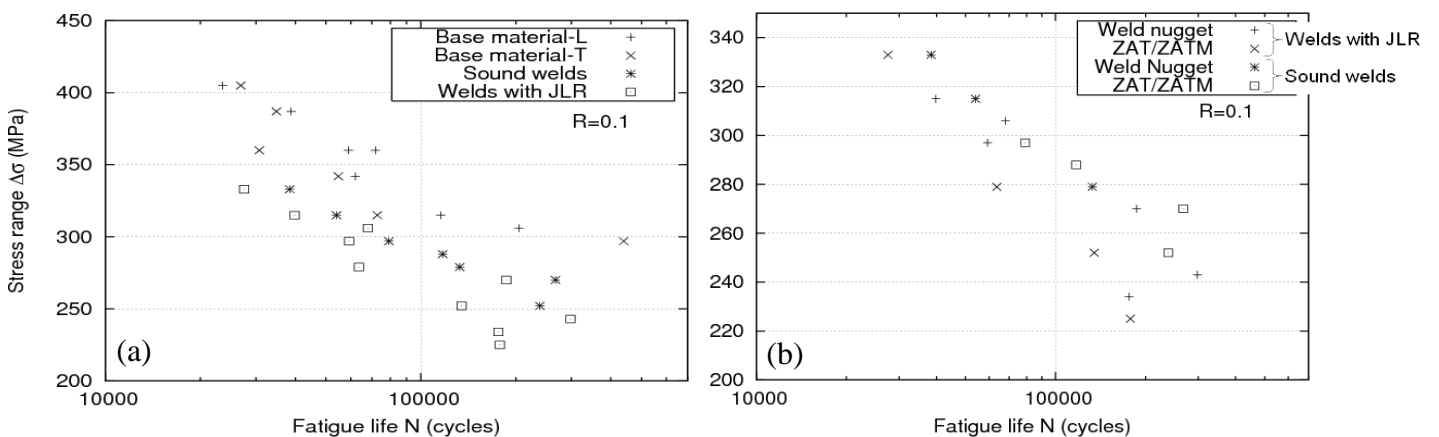


Fig. 8: (a) S-N curves of the base material and welded specimens. (b) Link to fatigue crack initiation sites
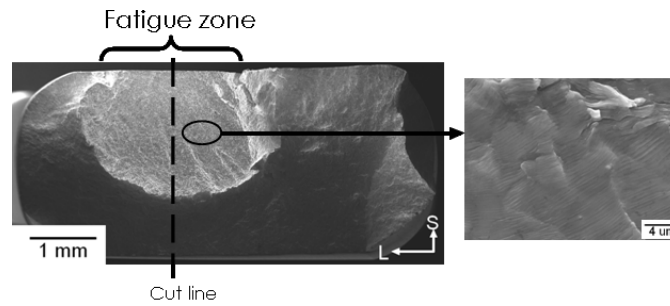
Fig. 9: SEM fractograph of a JLR-bearing specimen after fatigue testing. Fatigue striations are evidenced at higher magnification on the right



Fig. 10: Light optical micrographs of three representative welded fatigue specimens observed in the T-S plane for failure location (a) in weld nugget, (b) in TMAZ/HAZ, (c) next to the JLR. The JLR line has been redrawn for clarity in both three micrographs. Advancing side on the right

## DISCUSSION

The present experimental results show only a slight reduction in fatigue strength for a lifetime of $10^5$ cycles, for the chosen experimental parameters, for the JLR-free and JLR-bearing welds compared to the base material (about 10% and 15%, respectively). Location of fracture initiation is hardly affected by the presence of JLR. For the specimens that failed close to the JLR (30%) no reduction in fatigue lifetime could be evidenced in comparison with JLR-bearing specimens that failed at other locations.

The reduction in tensile properties such as yield strength is much more pronounced between welds and base material than the reduction in fatigue strength. This means that for all maximum stress levels chosen for fatigue tests, the welded material markedly deformed plastically during the first quarter of the first cycle, so that a prestrained material was subsequently tested. In particular, residual tensile stresses that have been identified in the WN [4, 20] are expected to be redistributed during the first fatigue cycle. On the other hand, the fatigue specimen elongates plastically and inhomogeneously during the first cycle and the geometry of the specimen is changed for the subsequent cycles.

For the present testing conditions (R=0.1), the material is loaded under tension during the entire cycle. If the plastically strained part of the weld hardened through kinematic hardening and if the material was loaded under tension-compression, the fatigue lifetime of the weld might be substantially lower, as the material would undergo macroscopic plastic deformation during each cycle. Due to the material thickness, 3.1 mm, it would be very difficult to perform tension-compression tests using the current test set-up because of buckling problems. Testing of the material through bending and fully reversed loading (R=-1) might be a way to assess this effect experimentally.

Due to the geometry of the weld zones and the inclined orientation of the weakest zone (TMAZ), plastic deformation during the first quarter of the first cycle may lead to compressive residual stresses that may be beneficial for the fatigue lifetime of the weld. Further measurements of the hardening behaviour of the different weld zones in the first quarter of the first cycle are necessary to better understand the weld behaviour.

6

**CONCLUSIONS**

In this study, an experimental investigation of the mechanical and fatigue properties of 2198 alloy in T851 condition, JLR-free and JLR-bearing friction stir welds has been carried out leading to the following conclusions:
- There is a strong influence of FSW on tensile properties since the yield strength and tensile strength of friction stir welds are reduced respectively by 45% and 22% compared to those of the base material.
- The weld microhardness profile shows a weak zone in which a decrease of 50 HV0.1 is observed compared to the value in the base material.
- The difference between the fatigue strength at $10^5$ cycles (R=0.1) of JLR-free welds and the base material is less pronounced (only 10%). Welds deform plastically, at least during the first cycle.
The effect of the JLR defect on the fatigue properties seems to be low since a reduction by only 15% of the fatigue strength at $10^5$ cycles was observed compared to the base material. Moreover, only in one third of specimens fatigue crack initiation took place close to the JLR defect and did even not seem to induce any reduction in fatigue lifetime in these cases.


**ACKNOWLEDGEMENTS**

**REFERENCES**

[1]     Shukla, A.K.; Baeslack, W. A.:
        Study of microstructural evolution in friction-stir welded thin-sheet Al-Cu-Li alloy using transmission-electron microscopy
        Scripta Materialia, 56(2007) No.6, pp. 513-516
[2]     Fonda, R.W.; Bingert, J.F.; Colligan, K.J.:
        Development of grain structure during friction stir welding
        Scripta Materialia, 51(2004) No.3, pp.243-248
[3]     Steglich, D.; Wafai, H.; Brocks, W.:
        Anisotropic deformation and damage in aluminium 2198 T8 sheets
        International Journal of Damage Mechanics, 00 (2009), pp.1-22
[4]     Bussu, G.; Irving, P.E.:
        The role of residual stress and heat a_ected zone properties on fatigue crack propagation in friction stir welded 2024-T351 aluminium joints
        International Journal of Fatigue, 25(2003) No.1, pp.77-88
[5]     Jata, K.V.;  Sankaran, K.K.; Ruschau, J.J.:
        Friction-stir welding effects on microstructure and fatigue of aluminum alloy 70 50-T7451. Metallurgical and Materials Transactions, 31(2000) No.9, pp.2181-2192
[6]     John, R.; Jata, K.V.; Sadananda; K.:
        Residual stress effects on near-threshold fatigue crack growth in friction stir welds in aerospace alloys International Journal of Fatigue, 25(2003) No.9-11, pp.939-948
[7]     Di, S.; Yang, X.; Luan, G.; Jian, B.:
        Comparative study on fatigue properties between AA2024-T4 friction stir welds and base materials

Materials Science and Engineering: A, 435-436 (2006), pp.389-395

[8] Sato, Y.S.; Takauchi, H.; Park, S.H.C.; Kokawa H.:
Characteristics of the kissing-bond in friction stir welded al alloy 1050. Materials Science and Engineering A-Structural Materials Properties Microstructure and Processing, 405 (2005) No.1-2, pp.333-338

[9] Chen, H. B.; Yan, K.; Lin, T.; Chen, S.B.; Jiang, C.Y.; Zhao, Y.:
The investigation of typical welding defects for 5456 aluminum alloy friction stir welds Materials Science and Engineering A433 (2006) No.1-2, pp.64-69

[10] Uematsu, Y.; Tokaji, K.; Shibata, H.; Tozaki, Y.; Ohmune, T.:
Fatigue behaviour of friction stir welds without neither welding ash nor aw in several aluminium alloys International Journal of Fatigue 31(2009) No.10, pp.1443-1453

[11] Vugrin, T.; Schmucker, M.; Staniek, G.:
Root flaws of friction stir welds - an electron microscopy study.
Friction Stir Welding and Processing III, TMS, Warrendale PA (2005), 277-284.

[12] Dickerson, T.L.; Przydatek, J.:
Fatigue of friction stir welds in aluminium alloys that contain root flaws
International Journal of Fatigue, 25 (2003) No.12, pp.1399-1409

[13] Zhou, C. Z.; Yang, X. Q.; Luan, G.H.:
Effect of root flaws on the fatigue property of friction stir welds in 2024-T3 aluminum alloys
Materials Science and Engineering A418 (2006) No.1-2, pp.155-160

[14] Zhou, C.; Yang, X.; Luan, G.:
Effect of oxide array on the fatigue property of friction stir welds
Scripta Materialia, 54 (2006) No.8, pp.1515-1520

[15] Zhou, C.Z.; Yang, X.Q.; Luan, G.H.:
Effect of kissing bond on fatigue behavior of friction stir welds on al 5083 alloy
Journal of Materials Science, 41 (2006) No.10, pp.2771-2777

[16] ASTM E 466
Standard practice for conducting force controlled constant amplitude axial fatigue tests of metallic materials, 2007.

[17] Denquin, A.; Allehaux, D.; Lapasset, G.; Ostersehlte, H.:
Microstructural phenomena of fsw joints: friction stir welding behaviour of 2098 type alloys and resulting weld properties
Proc. 11th International Conference on aluminium alloys, Aachen, Germany, 2008, pp.1939-1944

[18] Pouget, G.; Reynolds, A.P.:
Residual stress and microstructure effects on fatigue crack growth in AA2050 friction stir welds
International Journal of Fatigue, 30 (2008) No.3, pp.463-472

[19] Cavaliere, P.; De Santis, A.; Panella, F.; Squillace, A. :
Effect of anisotropy on fatigue properties of 2198 Al-Li plates joined by friction stir welding
Engineering Failure Analysis, 16 (2009) No.6, pp.1856-1865

[20] Peel, M.; Steuwer, A.; Preuss, M.; Withers, P.J.:
Microstructure, mechanical properties and residual stresses as a function of welding speed in aluminium AA5083 friction stir welds
Acta Materialia, 51(2003), No.16, pp.4791-4801

**Corresponding author:** thomas.le_jolu@ensmp.fr